



## OPEN

SUBJECT AREAS:  
ION CHANNELS IN THE  
NERVOUS SYSTEM  
HEPATOTOXICITYReceived  
1 September 2014Accepted  
24 November 2014Published  
15 December 2014Correspondence and  
requests for materials  
should be addressed to  
J.J.Z.  
(zhengjijian626@  
sina.com) or W.F.Y.  
(ywf808@sohu.com)\* These authors  
contributed equally to  
this work.

# Bilirubin Modulates Acetylcholine Receptors In Rat Superior Cervical Ganglionic Neurons In a Bidirectional Manner

Chengmi Zhang<sup>1,2\*</sup>, Zhenmeng Wang<sup>1\*</sup>, Jing Dong<sup>3</sup>, Ruirui Pan<sup>1</sup>, Haiibo Qiu<sup>1</sup>, Jinmin Zhang<sup>1</sup>, Peng Zhang<sup>4</sup>, Jijian Zheng<sup>3</sup> & Weifeng Yu<sup>1</sup>

<sup>1</sup>Department of Anesthesiology, Eastern Hepatobiliary Surgery Hospital, the Second Military Medical University, Shanghai, China, <sup>2</sup>Department of Anesthesiology, Xinhua Hospital, Shanghai Jiaotong University, Shanghai, China, <sup>3</sup>Department of Anesthesiology, Shanghai First People's Hospital, Shanghai Jiaotong University, Shanghai, China, <sup>4</sup>Department of Clinical Diagnosis, Changhai Hospital, the Second Military Medical University, Shanghai, China.

Autonomic dysfunction as a partial contributing factor to cardiovascular instability in jaundiced patients is often associated with increased serum bilirubin levels. Whether increased serum bilirubin levels could directly inhibit sympathetic ganglion transmission by blocking neuronal nicotinic acetylcholine receptors (nAChRs) remains to be elucidated. Conventional patch-clamp recordings were used to study the effect of bilirubin on nAChRs currents from enzymatically dissociated rat superior cervical ganglia (SCG) neurons. The results showed that low concentrations (0.5 and 2  $\mu\text{M}$ ) of bilirubin enhanced the peak ACh-evoked currents, while high concentrations (3 to 5.5  $\mu\text{M}$ ) of bilirubin suppressed the currents with an  $\text{IC}_{50}$  of  $4 \pm 0.5$   $\mu\text{M}$ . In addition, bilirubin decreased the extent of desensitization of nAChRs in a concentration-dependent manner. This inhibitory effect of bilirubin on nAChRs channel currents was non-competitive and voltage independent. Bilirubin partly improved the inhibitory effect of forskolin on ACh-induced currents without affecting the action of H-89. These data suggest that the dual effects of enhancement and suppression of bilirubin on nAChR function may be ascribed to the action mechanism of positive allosteric modulation and direct blockade. Thus, suppression of sympathetic ganglionic transmission through postganglionic nAChRs inhibition may partially contribute to the adverse cardiovascular effects in jaundiced patients.

Hyperbilirubinemic patients are more likely to develop hypotension, bradycardia and blunted vascular response to blood loss and vasoactive agents during surgery and intensive care settings<sup>1-3</sup>. Hyperbilirubinemia is also associated with increased occurrences of postoperative renal failure and hemorrhagic shock<sup>3,4</sup>. Other than extracellular water depletion, defective vascular reactivity, subclinical myocardial dysfunction and systemic endotoxemia, cardiovascular autonomic dysfunction is also involved in cardiovascular instability<sup>5-9</sup>. Our recent study<sup>10</sup> further demonstrated that both sympathetic and vagal components of arterial baroreflex were depressed in jaundiced patients, which may partially explain the increased susceptibility of cardiovascular instability to the above-mentioned perioperative complications.

Arterial baroreceptor reflex is a very important neural mechanism for moment-to-moment negative feedback control of arterial blood pressure fluctuations<sup>11,12</sup>. This complex and refined reflex process consists of baroreceptors located mainly in the carotid arteries and aortic arch to sense arterial pressure changes, afferent inputs to the brain stem center, the central integration of the afferent inputs from baroreceptors, and efferent outputs to cardiac and vascular targets through vagal and sympathetic nerves. Theoretically, any component change in this reflex loop will affect the regulatory function of the cardiovascular system<sup>13,14</sup>. Superior cervical ganglion (SCG) is an important sympathetic ganglion for regulating the cardiovascular function by acetylcholine released from preganglionic neurons, the center of the sympathetic nerve system<sup>15</sup>. SCG not only transfers but integrates the information from the center of the sympathetic nerve system through fast synaptic transmission mediated by nAChRs in SCG<sup>16,17</sup>, in which the cholinergic mechanism plays an important role in modulating the vasodilation



and cardiac sympathetic activation in humans<sup>18,19</sup>. Finally, the nAChRs in SCG can regulate the function of the cardiovascular system.

Bilirubin is a neurotoxin that can cause multiple neurologic dysfunctions such as bilirubin encephalopathy and cardiovascular instability. However, the mechanism underlying this effect has not been clearly elucidated<sup>10,20</sup>. Previous studies<sup>21–23</sup> have suggested that bilirubin encephalopathy might relate to the modification of synaptic transmission induced by bilirubin. Whether bilirubin can also affect the synaptic transmission in the sympathetic nervous system and finally cause cardiovascular instability is unknown. We therefore speculated that bilirubin could also affect sympathetic ganglion transmission. The aim of the present study was to confirm this hypothesis by exploring the effect of bilirubin on nAChRs in rat SCG neurons using the whole cell patch-clamp technique, knowing that SCG neurons are more sensitive to be affected than pre- and post-ganglionic fibers.

## Results

### Bidirectional modulation of rat SCG nAChRs by bilirubin.

According to our previous study, ACh with 1.0  $\mu\text{M}$  atropine puffed onto rat SCG neurons could elicit a transient peak inward current followed by a gradual decrease at a holding potential of  $-60$  mV (as shown in Fig. 1). The peak amplitudes and desensitization rates of nAChRs currents both increased in a concentration-dependent manner. The peak amplitude induced by 100  $\mu\text{M}$  ACh was close to the maximum value, and the desensitization rate at 5 s remained relatively slow. Therefore, 100  $\mu\text{M}$  ACh was chosen as the standard concentration to study the effect of bilirubin on nAChRs currents. In addition, the result of the nAChRs antagonist experiment showed that 100  $\mu\text{M}$  hexamethonium bromide, a nAChRs antagonist, completely blocked the currents induced by 200  $\mu\text{M}$  acetylcholine, which supports the nAChRs-mediated current specificity in our study (as shown in Fig. 2).

Bilirubin puffed onto rat SCG neurons did not elicit any current at holding potential of  $-60$  mV, but bilirubin modulated the nAChRs currents bidirectionally (Fig. 3) ( $n=5$ , each). At low concentrations (0.5 and 2  $\mu\text{M}$ ), bilirubin increased the peak nAChRs currents induced by 100  $\mu\text{M}$  acetylcholine by  $113 \pm 30\%$  and  $69 \pm 22\%$  respectively, and decreased the extent of desensitization 5 s after ACh puff by  $37 \pm 3\%$  and  $35 \pm 10\%$ , respectively. At high concentrations (3, 4 and 5  $\mu\text{M}$ ), bilirubin suppressed the peak current by  $9 \pm 5\%$ ,  $36 \pm 9\%$  and  $73 \pm 5\%$  respectively, and decreased the desensitization rate by  $42 \pm 13\%$ ,  $49 \pm 11\%$  and  $94 \pm 4\%$  respectively (Fig. 3) ( $n=5$ ). To calculate the  $\text{IC}_{50}$  value of bilirubin-induced nAChRs current inhibition, the peak nAChRs current in the presence of bilirubin was normalized to the base current induced by 100  $\mu\text{M}$  ACh only. The  $\text{IC}_{50}$  and Hill slope for bilirubin was  $4 \pm 0.5$   $\mu\text{M}$  and 1.0 respectively ( $n=5$ ) (Fig. 4). However, our data

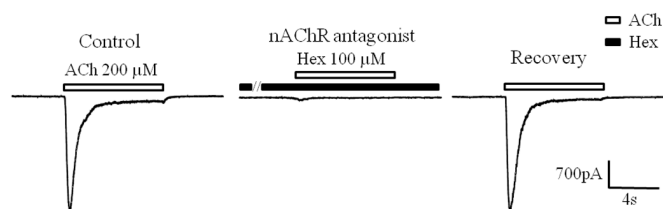


**Figure 2 | Specificity of nAChRs-mediated currents in SCG neurons.** Representative nAChR current traces evoked by ACh alone (control), coapplied with 100  $\mu\text{M}$  hexamethonium bromide, and ACh alone (recovery), respectively. 100  $\mu\text{M}$  hexamethonium bromide, a special nAChR antagonist, completely blocked the currents induced by 200  $\mu\text{M}$  acetylcholine.

demonstrated that both potentiation and suppression of nAChRs currents by bilirubin were accompanied with a decrease in nAChRs desensitization.

### Bilirubin voltage independently inhibits nAChR currents in rat SCG neurons.

To determine the possible mechanism of bilirubin-induced inhibition of nAChR, we further studied the effect of membrane potentials on bilirubin-induced inhibition of nAChR currents. Membrane potentials between  $-70$  mV and  $-20$  mV did not affect bilirubin-induced inhibition of the nAChR currents ( $p>0.05$ ), and 4.5  $\mu\text{M}$  bilirubin did not alter the reversal potential of nAChRs channel (0 mV) either (Fig. 5A). Both findings indicate that bilirubin suppressed the nAChR currents in rat SCG in a voltage-independent manner ( $n=5$ ) (Fig. 5B), which means that the binding sites of bilirubin to nAChRs may be distinct from acetylcholine-binding sites, knowing that orthosteric modulations are often affected by membrane potentials.

### Bilirubin non-competitively inhibits nAChRs currents in rat SCG neurons.

To further confirm our speculation, we explored the effect of bilirubin on the ACh concentration-response curve. As shown in Fig. 4, 4.0  $\mu\text{M}$  bilirubin significantly shifted the ACh-response curve to the right, and the  $\text{EC}_{50}$  and Hill slope for ACh with 4.0  $\mu\text{M}$  bilirubin were 356  $\mu\text{M}$  and 1.0 respectively. 4  $\mu\text{M}$  bilirubin suppressed nAChR currents induced by 100  $\mu\text{M}$  ACh. However, 4  $\mu\text{M}$  bilirubin greatly increased nAChR currents induced by 400  $\mu\text{M}$  and 800  $\mu\text{M}$  (Fig. 6). 200  $\mu\text{M}$  ACh just reversed the inhibition of the nAChR currents induced by 4.0  $\mu\text{M}$  bilirubin. However, 400  $\mu\text{M}$  and 800  $\mu\text{M}$  ACh not only reversed the inhibition of nAChR currents induced by 4.0  $\mu\text{M}$  bilirubin but the amplitude of the reversed peak of nAChR currents was much larger than that induced by 400  $\mu\text{M}$  and 800  $\mu\text{M}$  ACh puff alone, suggesting that the bilirubin-induced inhibition on nAChRs might be due to the non-competitive displacement of ACh at the

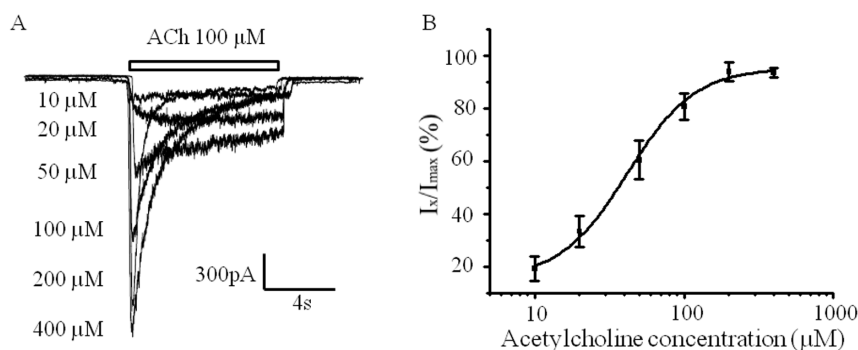


**Figure 1 | Dose-response curve of rat SCG nAChR currents.** (A), representative nAChR current traces evoked by 10, 20, 50, 100, 200 and 400  $\mu\text{M}$  ACh. (B), dose-response curve of nAChR currents fitted by nonlinear regression with logistic equation using Origin 8.0 software. Each data point represents mean  $\pm$  SEMs ( $n=9$ ).

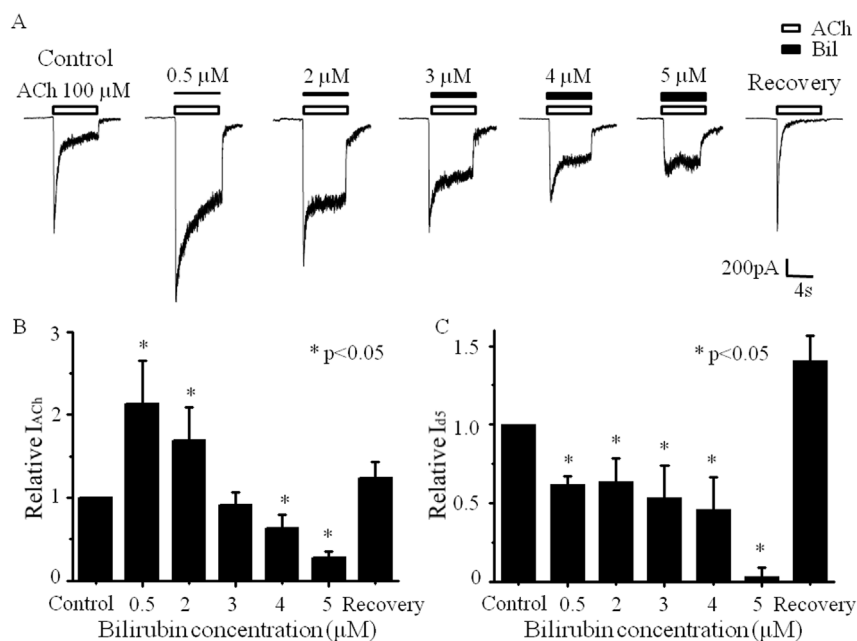


**Figure 3 | Bilirubin enhances and inhibits nAChR currents in rat SCG neurons in a dose-dependent manner.** (A) Representative traces of nAChR currents enhanced and inhibited by different concentrations of bilirubin (0.5, 2, 3, 4 and 5 μM). nAChR currents were activated by 100 μM ACh, and the duration of fast perfusion ACh by gravity was about 8 s. (B) The dose-response relationship for bilirubin on ACh-induced peak currents. The response rates of ACh-induced currents by bilirubin were normalized to the control response induced by 100 μM ACh. (C) The dose-response relationship for bilirubin on desensitization of nAChRs. Desensitization of nAChRs by bilirubin was normalized to the control response induced by 100 μM ACh. Each data point is expressed as means ± SEMs (n = 5).

acetylcholine-binding site, even though the possibility of inhibition by direct channel blockade, allosteric modulation or protein phosphorylation could not be ruled out.

**State-dependent blockade of nAChR channels by bilirubin.** To further clarify whether direct blockade of nAChR channels by bilirubin depended on different states of nAChRs, we first pre-applied 4.5 μM bilirubin and then co-applied 4.5 μM bilirubin with ACh, finding that pre-application of high concentrations of bilirubin further increased the inhibition of the peak nAChRs currents induced by co-application of bilirubin with ACh ( $53 \pm 5\%$  vs  $66 \pm 4\%$ , n = 6; P < 0.05), indicating that bilirubin preferred to bind to the closed stated nAChRs (Fig. 7).

**Inhibitory effect of cAMP on bilirubin-induced nAChR currents.** The inhibitory effect of protein phosphorylation on bilirubin-induced nAChR currents was then investigated. As shown in Fig. 5, 10 μM forskolin (a PKA activator that increases intracellular levels of cAMP) increased not only the nAChR currents but the inhibitory effect of

bilirubin on nAChR currents (Fig. 8). Although 1.0 μM H-89 (a PKA inhibitor that decreases intracellular levels of cAMP) alone also inhibited nAChR currents, 4 μM bilirubin reversed the inhibitory effect of H-89 on nAChRs currents (Fig. 9).

## Discussion

In the present study, we explored the effect of bilirubin on acetylcholine channels in rat SCG neurons and found that bilirubin modulated nAChRs in rat SCG neurons bidirectionally. Low concentrations (0.5 and 2 μM) of bilirubin increased the peak nAChR currents and decreased the extent of nAChR desensitization. However, high concentrations (3, 4 and 5 μM) of bilirubin decreased both the peak nAChR channel currents and the extent of nAChR desensitization. This inhibitory effect of bilirubin on nAChR channel currents was non-competitive and voltage independent, indicating that the suppression of AChR channel currents by bilirubin might be due to the allosteric modulation of nAChRs<sup>24,25</sup>. In addition, PKA signaling pathways were also involved in this inhibitory modulation of bilirubin on nAChRs channel currents.

Nicotinic acetylcholine receptors are so far the best characterized ion channels from the Cys-loop receptor superfamily with pentameric structures<sup>26</sup>. They are composed of the extracellular domain, transmembrane domain, the interface between them, and the cytoplasmic domain<sup>25</sup>. In addition to the classical orthosteric modulation of nAChRs by binding the N terminus of the extracellular domain of nAChRs at the interface between the extracellular and transmembrane domains, mounting studies have shown that nAChRs can also be modulated by allosteric modulation through binding site locations that are topographically distinct from the well-known orthosteric binding site<sup>25,26</sup>. Allosteric modulation includes negative allosteric modulation (NAM) and positive allosteric modulation (PAM)<sup>25</sup>. Negative allosteric modulators work like noncompetitive antagonists except that negative allosteric modulators bind to nonluminal sites instead of sites located in the ion channel like noncompetitive antagonists<sup>25</sup>. Positive allosteric modulators do not bind to the

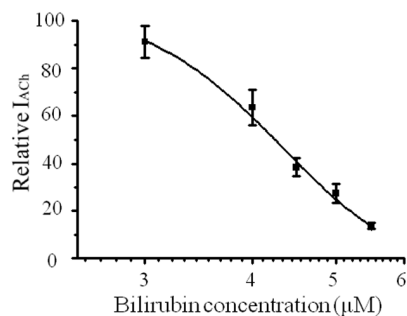


**Figure 4 | The dose-response curve for bilirubin.** The inhibitory rate of nAChR currents by bilirubin in SCG neurons was normalized to the control response induced by 100 μM ACh. Each data point is expressed as means ± SEMs (n = 5).

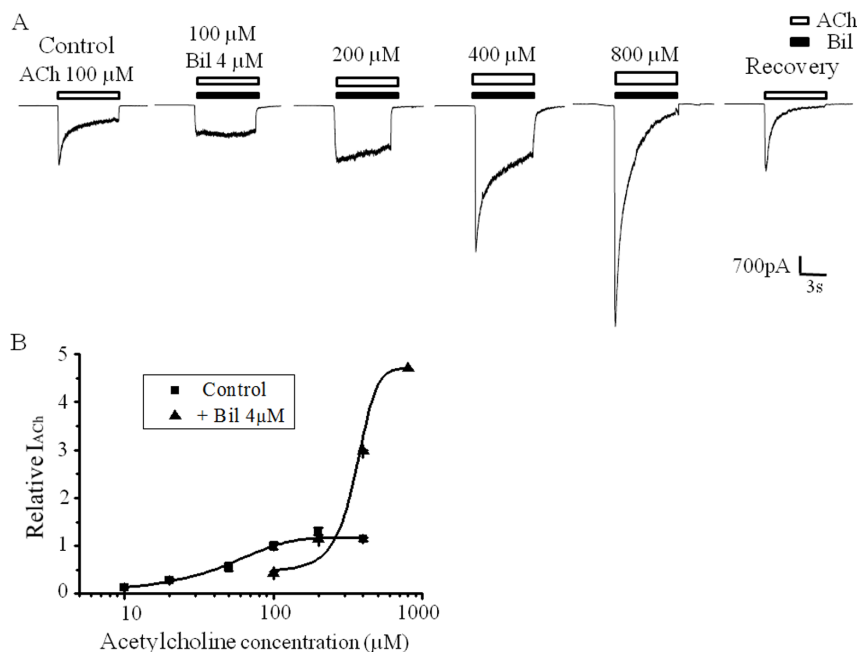


**Figure 5 | Voltage-independent suppression of nAChRs in rat SCG neurons.** (A) Current-voltage relationships of nAChRs induced by 100 μM ACh were derived from the ramp stimulation protocol (membrane potentials increased from  $-70$  mV to  $+30$  mV at a rate of 333 mV/s) in the presence (○) or absence (●) of 4.5 μM bilirubin. (B) There was no voltage dependency regarding the effect of 4.5 μM bilirubin on peak nAChRs currents. Each response was normalized to that without bilirubin at each membrane potential from  $-70$  mV to  $-20$  mV. All data points are expressed as means  $\pm$  SEMs ( $n = 5$ ).

orthosteric binding site either, but they can enhance the activity of agonists without changing the AChR desensitization properties (type I PAM) or decreasing the desensitization properties (type II PAM)<sup>25,27</sup>. However, long-time agonist activation by binding to orthosteric sites usually increases the desensitization rate of nAChRs<sup>25</sup>.

It was found in our study that low concentrations of bilirubin increased the peak amplitude of nAChR channel currents and decreased the nAChR desensitization rate, indicating that the potentiation of nAChR channel currents by low concentrations of bilirubin might be related to type II PAM. Unlike long-time agonist activation or competitive antagonists or noncompetitive antagonists, high concentrations of bilirubin decreased both the peak amplitude of nAChR channel currents and the nAChR desensitization rate. In addition, this inhibitory effect was voltage independent, indicating that the inhibition of nAChRs by bilirubin might be due to allosteric modulation instead of orthosteric modulation because the sites of orthosteric modulation mainly locate in the cell membrane and are subject to membrane potentials<sup>25,28</sup>. In addition, the decreased nAChR

desensitization rate during orthosteric modulation was usually followed by an increase in the peak amplitude of nAChR channel currents, while the increased nAChR desensitization rate was usually followed by a decrease in the peak amplitude of nAChR channel currents<sup>25</sup>. More complicatedly, we found that 4.0 μM bilirubin significantly reduced 100 μM ACh initiated nAChR currents. However, the nAChRs currents induced by high concentrations of ACh concentrations with 4.0 μM bilirubin were much larger than those induced by high concentrations of ACh concentrations alone, and the desensitization rate also changed from decrease to increase, suggesting that positive allosteric modulation or reactivation desensitized with nAChRs. Considering the variety of allosteric binding sites and multiple mechanisms, we speculated that type II PAM and/or reactivation of desensitized nAChRs together with steric blockade of the ion pore might contribute to the inhibition of nAChR currents induced by high-concentration bilirubin since steric blockade of the ion pore did not affect the desensitization of nAChRs<sup>11,24</sup>. More studies are still needed to further define the mechanism of nAChR modulation by bilirubin.

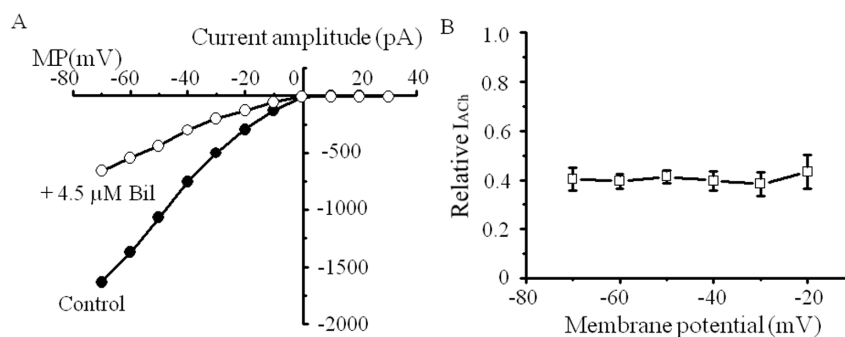


**Figure 6 | Curves represent the dose-responses of nAChR currents activated by ACh in the presence (▲) or absence (■) of 4 μM bilirubin.** All nAChR currents evoked by ACh in SCG neurons were normalized to that induced by 100 μM ACh alone (referred to as Relative I<sub>ACh</sub>). Administration of 4 μM bilirubin shifted the dose-responses of nAChR currents to the right, and markedly increased the potency and maximum efficacy of ACh (400 and 800 μM)-induced response. All data points are expressed as means  $\pm$  SEMs ( $n = 3$ ).

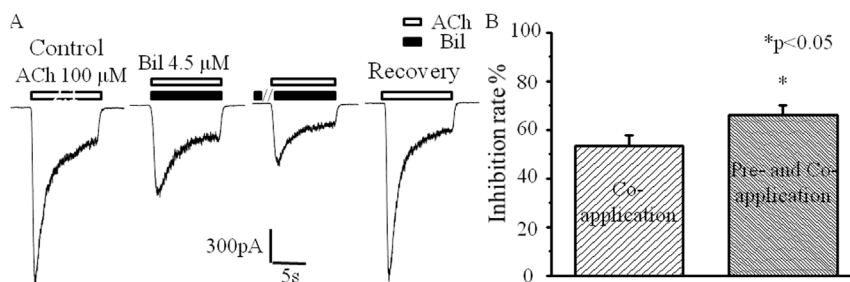


**Figure 7 | Enhanced inhibition of nAChRs by bilirubin pre-application.** (A), representative nAChR current traces evoked by ACh alone (control), coapplied with bilirubin, bilirubin pre-application, and ACh alone (recovery), respectively. (B), graph showing the percentage of current inhibition when 100  $\mu\text{M}$  ACh was coapplied with 4.5  $\mu\text{M}$  bilirubin with or without 4.5  $\mu\text{M}$  bilirubin preapplication. All data points are expressed as mean  $\pm$  SEMs ( $n = 6$ ).

Our findings at ion channel level of SCG neurons might shed some lights on the alteration of autonomic nerve activities in jaundiced patients. Our previous study<sup>10</sup> reported the evidence of BRS impairment in patients with obstructive jaundice. In addition, HRV as a very useful clinical tool to reflect the change of autonomic nerve activities was increased in newborn infants with mild/moderate jaundice and decreased in newborn infants with severe jaundice<sup>29</sup>. Other mechanisms underlying alteration of autonomic nerve activities in jaundiced patients need to be further explored.

Previous studies<sup>30,31</sup> suggest that bilirubin can modulate neurotransmitter release via presynaptic PKA activation and inhibit phosphorylation of the synaptic vesicle-associated protein synapsin I, eventually causing dysfunction of relative organs. Protein phosphorylation of the cytoplasmic domain of nAChRs can modulate the kinetics of receptor gating<sup>32,33</sup>. In our study, forskolin (PKA activator) not only inhibited nAChR currents but increased the inhibitory effect of bilirubin on nAChR currents. H-89 (a PKA inhibitor) alone inhibited nAChR currents. However, 4  $\mu\text{M}$  bilirubin reversed the inhibitory effect of H-89 on nAChR currents, suggesting that the PKA pathway might play a role in hyperbilirubinemia-mediated

dysfunction of the cardiovascular system. Previous studies<sup>30</sup> showed that PKA regulated the synaptic transmission through phosphorylation of presynaptic proteins, various ion channels, and certain neurotransmitter receptors. Therefore, the exact action mechanism of bilirubin on nAChRs via the PKA pathway is extremely interesting and warrants further investigation.

The neurotoxicity of bilirubin is determined by the free fraction of unconjugated bilirubin that is not bound to plasma proteins<sup>34,35</sup>. Unbound bilirubin concentrations can reach a level as high as  $3 \times 10^{-6}$  M during severe human hyperbilirubinemia<sup>20</sup> and free bilirubin levels of  $7 \times 10^{-8}$  M can induce apoptosis in cultured cortical neurons<sup>36</sup>. In the present study, we applied unconjugated bilirubin to isolated SCG neurons without any plasma proteins, and therefore the concentrations of bilirubin that we used in this study are clinically relevant.

Our study may partially explain the important mechanism of reduction in sympathetic baroreflex sensitivity in patients with obstructive jaundice. However, there are some limitations in our study. Bilirubin modulates several processes related to synaptic transmission, including neurotransmitter synthesis, release and

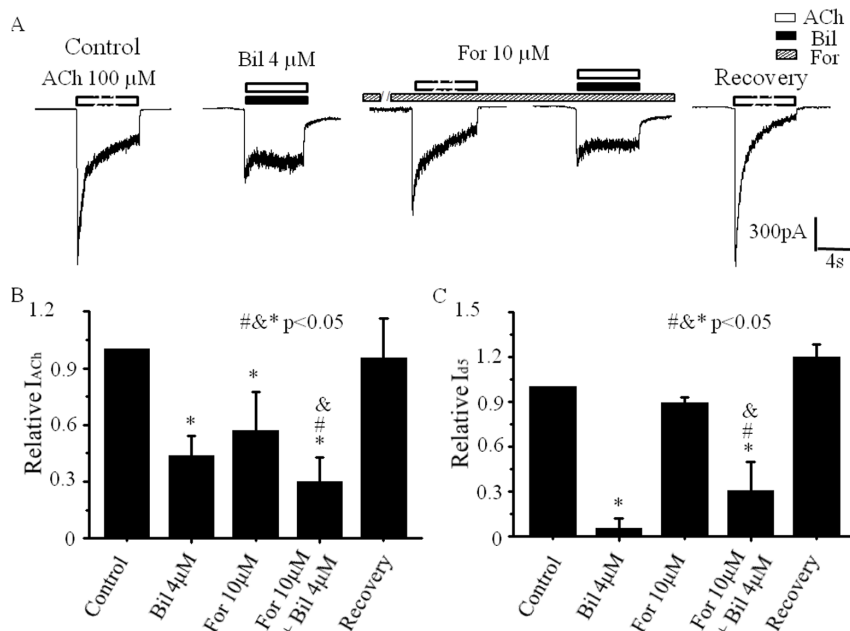


**Figure 8 | Bilirubin is involved in the cAMP and PKA pathway in suppressing nAChR currents.** The inhibitory effect of bilirubin on nAChR currents persisted in the presence of 10  $\mu\text{M}$  forskolin. (A) Representative traces of nAChR currents inhibited by 4  $\mu\text{M}$  bilirubin persisted in the presence of 10  $\mu\text{M}$  forskolin. (B) The dose-response relationship for bilirubin on ACh-induced peak currents persisted in the presence of 10  $\mu\text{M}$  forskolin. The response rates of ACh-induced currents by bilirubin were normalized to the control response induced by 100  $\mu\text{M}$  ACh. (C) The dose-response relationship for bilirubin on desensitization of nAChR persisted in the presence of 10  $\mu\text{M}$  forskolin. Desensitization of nAChRs by bilirubin was normalized to the control response induced by 100  $\mu\text{M}$  ACh. Each data point is expressed as means  $\pm$  SEMs ( $n = 5$ ).

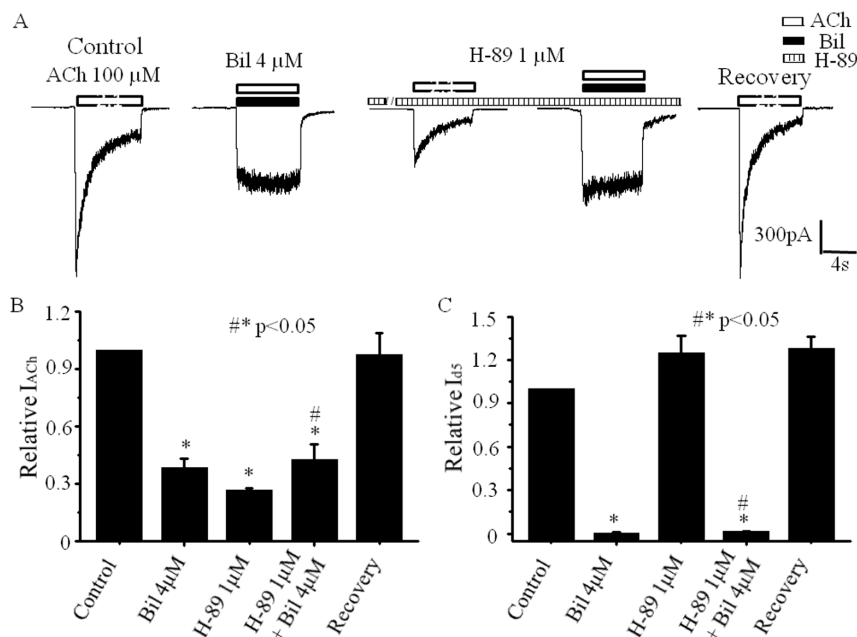


**Figure 9 | The inhibitory effect of bilirubin on nAChR currents persisted in the presence of 1  $\mu\text{M}$  H-89.** (A) Representative traces of nAChR currents inhibited by 4  $\mu\text{M}$  bilirubin persisted in the presence of 1  $\mu\text{M}$  H-89. (B) The dose-response relationship for bilirubin on ACh-induced peak currents persisted in the presence of 1  $\mu\text{M}$  H-89. The response rates of ACh-induced currents by bilirubin were normalized to the control response induced by 100  $\mu\text{M}$  ACh. (C) The dose-response relationship for bilirubin on desensitization of nAChR persisted in the presence of 1  $\mu\text{M}$  H-89. Desensitization of nAChRs by bilirubin was normalized to the control response induced by 100  $\mu\text{M}$  ACh. Each data point is expressed as means  $\pm$  SEMs ( $n = 5$ ).

uptake<sup>21</sup>, and directly inhibits both exocytotic release and vesicular storage of catecholamines<sup>37</sup>. However, our study only focused on the effect of bilirubin on nAChRs in isolated SCG neurons without simultaneously studying the effect of ACh release from preganglionic sympathetic fibers and catecholamine release from postganglionic sympathetic fibers. We did not study the effect of bilirubin on nAChR subtypes or other ion channels. In addition, the positive allosteric modulation and direct blockade of SCG nAChR channels by high concentrations of bilirubin were mainly based on electrophysiological studies. The specific allosteric binding sites remain unclear. Molecular docking combined with point mutation techniques are needed to further clarify the allosteric binding sites and radioligand binding in future studies. Finally, the species difference might also affect our results. Therefore, further work is necessary to elaborate the precise mechanism of nAChR allosteric modulation by bilirubin, knowing that compounds binding to several sites with different affinities may produce positive and negative AChR modulations, such as  $\text{Zn}^{2+}$  modulation of AChRs with the manner of positive and negative allosteric modulations by binding to two different domains<sup>38</sup>.

In conclusion, low concentrations of bilirubin enhanced the function of nAChRs at SCG neurons, while high concentrations of bilirubin inhibited the function of nAChRs at SCG neurons. This bidirectional modulation of nAChRs at SCG neurons by bilirubin might be due to positive allosteric modulation or reactivated desensitized AChRs together with direct channel blockade. Suppression of sympathetic ganglionic transmission through postganglionic nAChR inhibition might partially contribute to the adverse cardiovascular effect in jaundiced patients.

## Methods

**Isolation of single rat SCG neurons.** All experiments were performed in accordance with the National Institutes of Health guidelines and regulations. The animal protocol was approved by Shanghai First People's Hospital Animal Care and Use Committee in accordance with the Guide for the Care and Use of Laboratory Animals published by the US National Institutes of Health (National Institutes of Health Publication No. 85-23, revised 1996). Neonatal Sprague-Dawley (SD) rats were obtained from the Experimental Animal Department of Shanghai First People's Hospital (Shanghai, China).

Neonatal SD rats were terminally anesthetized with  $\text{CO}_2$  and immediately decapitated. Neurons from rat SCG were freshly dissociated as described previously<sup>39,40</sup>. Briefly, both sides of SCG were acutely dissociated from SD rats aged 4–6 days, and each SCG was sliced into 2–4 sections in ice-cold well-oxygenated bathing solution using a razor blade. The sections were then transferred into well-oxygenated bath solution containing pronase E (1.5 mg/ml, Sigma Chemical Co., Saint Louis, USA), collagenase (1.0 mg/ml, Worthington Biochemical Co, Lakewood, NJ) and DNaseI (0.1 mg/ml, Sigma Chemical Co., Saint Louis, USA) for 40 min at 31.5°C. After digestion, the tissue sections were washed 3 times with oxygenated bath solution, and SCG neurons were mechanically dispersed by triturating the SCG fragments using a series of fire polished Pasteur pipettes with decreasing tip diameter. The cell suspension was then maintained in oxygenated bath solution at room temperature for electrophysiological recording. All experiments were performed within 6 h after isolation.

**Electrophysiological recording.** Conventional whole-cell voltage-clamp recording was performed at room temperature (22–25°C using HEKA EPC-10 amplifiers and Patch-Master software (HEKA Elektronik, Germany)<sup>41</sup>. Patch pipettes were pulled from 1.5-mm diameter thin-walled borosilicate glass capillaries (Sutter Instruments Co., Novato, CA, USA) using the Flaming/Brown micropipette puller P97 (Sutter Instruments Co., Novato, CA, USA), and had a resistance of 2–4 M $\Omega$  when filled with pipette solution. After forming a “gigaseal,” the membrane was ruptured with a gentle suction to form the whole cell voltage clamp. Once the whole cell configuration was established, the membrane potential was held at  $-60$  mV, and the series resistance compensation was adjusted to 50–75%. If the series resistance exceeded 10 M $\Omega$ , the recording was discarded. All currents were low-pass Bessel filtered at 1 kHz, digitized at 5 kHz, and were stored on a computer for subsequent analysis.

**Solutions and drugs.** The pipette internal solution contained (in mM): KCl 150,  $\text{MgCl}_2$  2.0, EGTA 5.0, HEPES 10,  $\text{Na}_2\text{ATP}$  2.0, pH 7.2. The standard external solution contained (in mM): NaCl 130, KCl 5.0,  $\text{MgCl}_2$  1.0,  $\text{CaCl}_2$  2.0, Glucose 10, Sucrose 10, HEPES 10, pH 7.4. The bath solution contained (in mM): NaCl 130, KCl 5.0,  $\text{MgCl}_2$  1.0,  $\text{CaCl}_2$  2.0, Glucose 20, Sucrose 10, HEPES 10, pH 7.4.

Drugs used in these experiments were unconjugated bilirubin, acetylcholine, atropine, forskolin, and N-mo-5-isoquinolinesulfonamide dihydrochloride (H-89) (Sigma, Saint Louis, USA). The bilirubin stock solution consisted of  $10^{-3}$  M bilirubin dissolved in 0.1 M NaOH and was stored in single-use aliquots in the dark at  $-20^\circ\text{C}$ . Aliquots were diluted in the final solution prior to application and protected from light to avoid photosensitivity. All drugs were diluted in the standard external solution to their respective experimental concentrations. One micromolar atropine sulfate was added to the standard external solution to block mAChR currents, while the other drugs were applied using the Y-tube method<sup>39</sup>.

**Data analysis.** All data were analyzed using Patch-Master and Origin 8 (Origin-Lab, Northampton, MA, USA), and are presented as mean  $\pm$  SEMs. Statistical significance



was assessed using one-way analysis of variance (ANOVA) and paired two-tailed Student's *t*-test.  $P < 0.05$  was considered significant.

The concentration-response relationship of nAChRs currents was fitted by non-linear regression with the following logistic equation:  $Y = \text{Bottom} + (\text{Top} - \text{Bottom}) / (1 + 10^{-(\text{Log EC}_{50} - X) \cdot \text{Hill Slope}})$ , where  $Y$  is the normalized response,  $X$  is the logarithm of concentration, and  $\text{EC}_{50}$  is referred to as the half maximal effective concentration. This equation was also used for the effect of bilirubin on ACh-induced currents, where  $\text{EC}_{50}$  was replaced by the half maximal inhibitory concentration ( $\text{IC}_{50}$ )<sup>42</sup>. The extent of desensitization of nAChRs currents was quantified as the percent decay of the ACh-induced current from the peak at  $t = 5$  s,  $I_{45}$ , according to the equation  $I_{45} = (I_{\text{peak}} - I_5) / I_{\text{peak}} \times 100\%$ , where  $I_{\text{peak}}$  is the peak ACh induced current, and  $I_5$  denotes the current measured 5 s after ACh or ACh and bilirubin co-application<sup>43</sup>.

The inhibitory effect of bilirubin on nAChRs was assessed by acquiring the relationship between current and voltage as described by Haghghi et al.<sup>44</sup>. Briefly, a ramp stimulation protocol was used to increase the membrane potential from  $-70$  mV to  $+30$  mV at a rate of  $333$  mV/s. Current-voltage (*I-V*) curves were then obtained by subtracting the control current from the current during the ACh alone or ACh and bilirubin co-application. Relative nAChRs currents (IACH) were then normalized to that without bilirubin at each membrane potential.

- Yang, L. Q. et al. A clinical prospective comparison of anesthetics sensitivity and hemodynamic effect among patients with or without obstructive jaundice. *Acta Anaesthesiol Scand* **54**, 871–877 (2010).
- Bansal, V. & Schuchert, V. D. Jaundice in the intensive care unit. *Surg Clin North Am* **86**, 1495–1502 (2006).
- Wang, L. & Yu, W. F. Obstructive jaundice and perioperative management. *Acta Anaesthesiol Taiwan* **52**, 22–29 (2014).
- Green, J. & Better, O. S. Systemic hypotension and renal failure in obstructive jaundice-mechanistic and therapeutic aspects. *J Am Soc Nephrol* **5**, 1853–1871 (1995).
- Sitges-Serra, A. et al. Body water compartments in patients with obstructive jaundice. *Br J Surg* **79**, 553–556 (1992).
- Utkan, Z. N., Utkan, T., Sarioglu, Y. & Gonullu, N. N. Effects of experimental obstructive jaundice on contractile responses of dog isolated blood vessels: role of endothelium and duration of bile duct ligation. *Clin Exp Pharmacol Physiol* **27**, 339–344 (2000).
- Padillo, J. et al. Improved cardiac function in patients with obstructive jaundice after internal biliary drainage: hemodynamic and hormonal assessment. *Annals of Surgery* **234**, 652–656 (2001).
- Papakostas, C. et al. Endotoxemia in the portal and the systemic circulation in obstructive jaundice. *Clin Exp Med* **3**, 124–128 (2003).
- Ren, H. M. et al. In vivo and ex vivo effects of propofol on myocardial performance in rats with obstructive jaundice. *BMC Gastroenterol* **11**, 144 (2011).
- Song, J. G. et al. Baroreflex sensitivity is impaired in patients with obstructive jaundice. *Anesthesiology* **111**, 561–565 (2009).
- Eckberg, D. L. & Sleight, P. [Introduction, History and Baroreflex anatomy] *Human Baroreflexes in Health and Disease*. [Eckberg D. L. & Sleight P. (ed.)] [3–57] (Oxford, England, 1992).
- Phillips, A. A. et al. Increased central arterial stiffness explains baroreflex dysfunction in spinal cord injury. *J Neurotrauma* **31**, 1122–1128 (2014).
- Chesterton, L. J. & McIntyre, C. W. The assessment of baroreflex sensitivity in patients with chronic kidney disease: implications for vasomotor instability. *Curr Opin Nephrol Hypertens* **14**, 586–591 (2005).
- Latson, T. W. et al. Autonomic reflex dysfunction in patients presenting for elective surgery is associated with hypotension after anesthesia induction. *Anesthesiology* **80**, 326–337 (1994).
- Alkadhi, K. A., Alzoubi, K. H. & Aleisa, A. M. Plasticity of synaptic transmission in autonomic ganglia. *Prog Neurobiol* **75**, 83–108 (2005).
- De Biasi, M. Nicotinic mechanisms in the autonomic control of organ systems. *J Neurobiol* **53**, 568–579 (2002).
- David, R. et al. Biochemical and functional properties of distinct nicotinic acetylcholine receptors in the superior cervical ganglion of mice with targeted deletions of nAChR subunit genes. *Eur J Neurosci* **31**, 978–993 (2010).
- Lepori, M. et al. Interaction between cholinergic and nitrergic vasodilation: a novel mechanism of blood pressure control. *Cardiovasc Res* **51**, 767–772 (2001).
- Sartori, C., Lepori, M. & Scherrer, U. Interaction between nitric oxide and the cholinergic and sympathetic nervous system in cardiovascular control in humans. *Pharmacol Ther* **106**, 209–220 (2005).
- Lee, Y. K. et al. The significance of measurement of serum unbound bilirubin concentrations in high-risk infants. *Pediatr Int* **51**, 795–799 (2009).
- Ochoa, E. L. et al. Interactions of bilirubin with isolated presynaptic nerve terminals: functional effects on the uptake and release of neurotransmitters. *Cell Mol Neurobiol* **13**, 69–86 (1993).
- Chang, F. Y., Lee, C. C., Huang, C. C. & Hsu, K. S. Unconjugated bilirubin exposure impairs hippocampal long-term synaptic plasticity. *PLoS One* **4**, e5876 (2009).
- Shi, H. B. et al. Bilirubin potentiates inhibitory synaptic transmission in lateral superior olive neurons of the rat. *Neurosci Res* **55**, 161–170 (2006).
- Olivera-Bravo, S., Ivorra, I. & Morales, A. Diverse inhibitory actions of quaternary ammonium cholinesterase inhibitors on Torpedo nicotinic ACh receptors transplanted to Xenopus oocytes. *Br J Pharmacol* **151**, 1280–1292 (2007).
- Arias, H. R. Positive and negative modulation of nicotinic receptors. *Adv Protein Chem Struct Biol* **80**, 153–203 (2010).
- Papke, R. L. Merging old and new perspectives on nicotinic acetylcholine receptors. *Biochem Pharmacol* **89**, 1–11 (2014).
- Williams, D. K., Wang, J. & Papke, R. L. Positive allosteric modulators as an approach to nicotinic acetylcholine receptor-targeted therapeutics: advantages and limitations. *Biochem Pharmacol* **82**, 915–930 (2011).
- Jackson, C., Bermudez, I. & Beadle, D. J. Pharmacological properties of nicotinic acetylcholine receptors in isolated *Locusta migratoria* neurones. *Microsc Res Tech* **56**, 249–255 (2002).
- Guo, Z. M., Liu, F., Zhou, C. F. & Du, Z. F. Influence of newborn jaundice on heart rate variability and its clinical significance. *Clin J Med Offic* **38**, 592–594 (2010).
- Li, C. Y. et al. Protein kinase A and C signaling induces bilirubin potentiation of GABA/glycinergic synaptic transmission in rat ventral cochlear nucleus neurons. *Brain Res* **1348**, 30–41 (2010).
- Hansen, T. W., Bratlid, D. & Walaas, S. I. Bilirubin decreases phosphorylation of synapsin I, a synaptic vesicle-associated neuronal phosphoprotein, in intact synaptosomes from rat cerebral cortex. *Pediatr Res* **23**, 219–223 (1988).
- Cho, C. H. et al. Rapid upregulation of alpha7 nicotinic acetylcholine receptors by tyrosine dephosphorylation. *J Neurosci* **25**, 3712–3723 (2005).
- Araud, T., Wonnacott, S. & Bertrand, D. Associated proteins: The universal toolbox controlling ligand gated ion channel function. *Biochem Pharmacol* **80**, 160–169 (2010).
- Hulzebos, C. V. et al. Usefulness of the bilirubin/albumin ratio for predicting bilirubin-induced neurotoxicity in premature infants. *Arch Dis Child Fetal Neonatal* **93**, F384–388 (2008).
- Daood, M. J., McDonagh, A. F. & Watchko, J. F. Calculated free bilirubin levels and neurotoxicity. *J Perinatol* **29** Suppl 1, S14–19 (2009).
- Silva, R. F., Rodrigues, C. M. & Brites, D. Bilirubin-induced apoptosis in cultured rat neural cells is aggravated by chenodeoxycholic acid but prevented by ursodeoxycholic acid. *J Hepatol* **34**, 402–408 (2001).
- Hansen, T. W., Mathiesen, S. B., Sefland, I. & Walaas, S. I. Bilirubin inhibits Ca<sup>2+</sup>-dependent release of norepinephrine from permeabilized nerve terminals. *Neurochem Res* **24**, 733–738 (1999).
- Moroni, M. et al. Non-agonist-binding subunit interfaces confer distinct functional signatures to the alternate stoichiometries of the alpha4beta2 nicotinic receptor: an alpha4-alpha4 interface is required for Zn<sup>2+</sup> potentiation. *J Neurosci* **28**, 6884–6894 (2008).
- Uki, M., Nabekura, J. & Akaike, N. Suppression of the nicotinic acetylcholine response in rat superior cervical ganglionic neurons by steroids. *J Neurochem* **72**, 808–814 (1999).
- Zhang, C. M. et al. Competitive inhibition of the nondepolarizing muscle relaxant rocuronium on nicotinic acetylcholine receptor channels in the rat superior cervical ganglia. *J Cardiovasc Pharmacol* **63**, 428–433 (2014).
- Hamill, O. P. et al. Improved patch-clamp techniques for high-resolution current recording from cells and cell-free membrane patches. *Pflügers Arch* **391**, 85–100 (1981).
- Jonsson, M. et al. Activation and inhibition of human muscular and neuronal nicotinic acetylcholine receptors by succinylcholine. *Anesthesiology* **104**, 724–733 (2006).
- Tan, W., Du, C., Siegelbaum, S. A. & Role, L. W. Modulation of nicotinic AChR channels by prostaglandin E2 in chick sympathetic ganglion neurons. *J Neurophysiol* **79**, 870–878 (1998).
- Haghghi, A. P. & Cooper, E. Neuronal nicotinic acetylcholine receptors are blocked by intracellular spermine in a voltage-dependent manner. *J Neurosci* **18**, 4050–4062 (1998).

## Acknowledgments

This study was supported by the National Natural Science Foundation of China (Beijing, China) (Grant No. 81170427 to Wei-Feng Yu, Grant No. 81100312 to Zhen-Meng Wang, Grant No. 81271263 to Ji-Jian Zheng).

## Author contributions

C.Z., Z.W., J.Z. (Jijian Zheng), J.D. and W.Y. conceived and designed the project. C.Z., J.D., R.P., H.Q., J.Z. (Jinmin Zheng) and P.Z. performed all the experiments and prepared the figures. C.Z., Z.W. and J.Z. (Jijian Zheng) wrote the manuscript. All authors have reviewed the manuscript.

## Additional information

**Competing financial interests:** The authors declare no competing financial interests.

**How to cite this article:** Zhang, C. et al. Bilirubin Modulates Acetylcholine Receptors In Rat Superior Cervical Ganglionic Neurons In a Bidirectional Manner. *Sci. Rep.* **4**, 7475; DOI:10.1038/srep07475 (2014).



This work is licensed under a Creative Commons Attribution-NonCommercial-NoDerivs 4.0 International License. The images or other third party material in this article are included in the article's Creative Commons license, unless indicated otherwise in the credit line; if the material is not included under the Creative

Commons license, users will need to obtain permission from the license holder in order to reproduce the material. To view a copy of this license, visit <http://creativecommons.org/licenses/by-nc-nd/4.0/>